



Effect of Pulse Current on Shrinkage Stress and Distortion in Multipass GMA Welds of Different Groove Sizes

The pulsed gas metal arc process was found to be beneficial in reducing shrinkage stress and distortion in welds on 16-mm-thick HSLA steel

BY P. K. GHOSH, K. DEVAKUMARAN, AND A. K. PRAMANICK

ABSTRACT

Multipass butt joining of 16-mm-thick microalloyed high-strength low-alloy (HSLA) steel plates was carried out by gas metal arc welding (GMAW) with and without pulsed current on different sizes of conventional and narrow grooves. Effect of welding parameters, thermal behavior, and groove size on shrinkage stress, distortion, and bending stress were suitably measured or estimated in appropriate occasions. It was observed that the use of pulsed current with controlled parameters can improve the characteristics of the weld joint with respect to its distortion and stresses, especially in the case of suitable narrow groove welds. Influence of the concerned functions on the weld characteristics studied are appropriately correlated and discussed.

Introduction

The distortion and shrinkage stress giving rise to thermal straining of a weld joint largely results from differential contraction of the weld and neighboring base metal arising out of the cooling cycle of the welding process. The thermal strain produced along the direction of welding results from the longitudinal shrinkage,

P. K. GHOSH (prakgfmt@gmail.com), K. DEVAKUMARAN (devaa2001@gmail.com), and A. K. PRAMANICK (ajitpramanick@gmail.com) are with Department of Metallurgical & Materials Engineering, Indian Institute of Technology Roorkee, Roorkee, India.

whereas the strain produced in the component normal to the direction of welding is caused by the transverse shrinkage (Refs. 1–3). A combined stress resulting from the thermal strains reacting to develop internal forces causes weld distortion, commonly observed as bending (Refs. 1, 3). Welding distortion has a negative effect on the dimensional accuracy of assembly as well as external appearance and mechanical properties of the weld joint, which can add additional cost to rectify in commercial practices. Depending upon length of the weld, the linear bending stress may be due to longitudinal shrinkage (Refs. 1, 2). However, the transverse bending always remains significant in reference to plastic upsetting in the zone adjacent to the weld. As a consequence of the in-homogeneous permanent deformation of the weld and its adjacent area, some residual stresses develop in the weld joint (Refs. 4–6). The presence of residual stresses in the weld joint may adversely affect the fatigue, stress corrosion cracking, and fracture mechanics properties of the weld joint depending upon characteristics of the material (Refs. 5–8). Thus, a critical look into the development of shrinkage indulging distortion in welding depending upon the process, procedure, and parameter has always been felt

KEYWORDS

Welding Processes
Weld Groove Size
Weld Distortion
Shrinkage Stresses
Bending Stresses
Pulsed Current
GMAW

imperative to produce welds of superior quality. A significant amount of experiments and numerical analyses have been carried out for measurement and estimation of shrinkage and deformation of the weld joint, which explore basic understanding of this area (Refs. 9–11). But hardly any systematic work has been reported on estimation and measurement of welding deformation in thick plate with different sizes of weld grooves and welding parameters using the gas metal arc welding (GMAW) process. This is especially true in the case of pulsed current gas metal arc welding (GMAW-P), where the situation becomes more complex due to involvement of a relatively large number of simultaneously interactive pulse parameters, such as mean current (I_m), pulse current (I_p), base current (I_b), pulse time (t_p), base time (t_b), and pulse frequency (f) at different arc voltages (V). However, a solution to the critical control of pulse parameters for the desired operation of the GMAW-P process has been well addressed by considering a summarized influence of pulse parameters defined by a dimensionless hypothetical factor $\phi = (I_b/I_p) \times ft_b$ derived on the basis of energy balance concept (Refs. 5, 8, 12–14) where, t_b is expressed as $[(1/f) - t_p]$. Thus, the control of thermal and metal transfer behavior as well as efficiency of the process, which may largely depend on interactive pulsed parameters, can be accomplished in consideration of the factor ϕ .

In view of the above, an effort has been made in this work to estimate transverse shrinkage stress and bending stress by measurement of transverse shrinkage and distortion under different welding processes, procedures, and parameters during welding of 16-mm-thick controlled-rolled high-strength low-alloy (HSLA) steel plates. At a given heat input and weld groove size the effect of welding processes,

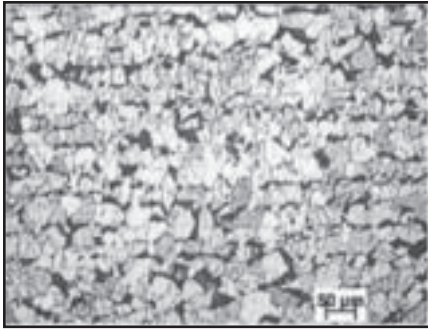


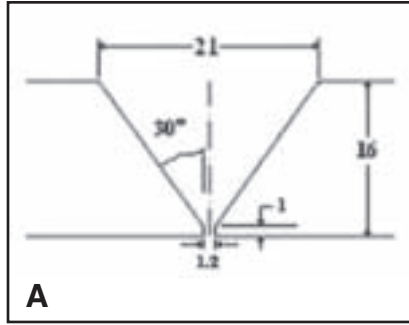
Fig. 1 — Typical microstructure of base metal.

procedures, and parameters on variation of estimated shrinkage stresses in the weld deposit causing bending of the weld joint were corroborated by the estimation of bending stresses developed in the weld joint through the measurement of plate bending during welding. This provides an opportunity to physically confirm the effect of various welding processes and procedures on the stress generation in the weld joint. These observations may be beneficial for using the GMAW-P process to produce desired weld quality, and also may form a basis for improvement in its automation.

Experimentation and Analysis

Welding

Controlled-rolled 16-mm-thick micro-alloyed HSLA steel plates of specification SAILMA-350 HI/SA533 grade having the chemical composition given in Table 1 were used in this work. Typical microstructure of the base metal is shown in Fig. 1. The plates in size of 110 × 110 mm were butt joint welded by multipass deposition technique using a single V-groove with an included angle of 60 deg, which conformed to AWS specification (Ref. 15), and also by using a suitably designed narrow groove with 11- and 8-mm groove openings, designated by NG-11 and NG-8, respectively, as schematically shown in Fig. 2A–C. The plates were welded by continuous current gas metal arc welding (GMAW) and pulsed current gas metal arc welding (GMAW-P) processes at direct current electrode positive (DCEP). The welding was performed by using 1.2-mm-diameter mild steel welding wire of



specification AWS/SFA 5.18ER-70S-6 under argon (99.97%) gas shielding at a flow rate of 16–18 L/min. During welding the distance between the nozzle to workpiece was maintained within 17–18 mm. A relatively long electrode extension was used to facilitate welding gun manipulation in the narrow groove for weld deposition with satisfactory root and groove wall fusion. Welding of the plates was carried out using semiautomatic welding with a mechanized welding gun travel. The details of the welding parameters used in this work are presented in Table 2. Prior to welding, the plates were preheated to about 125–130°C, and after each pass, the deposit was allowed to cool down to room temperature followed by reheating to maintain an interpass temperature similar to that of preheating for subsequent weld passes. The welding was carried out by rigid clamping of one side of the weld joint, where the other side of it was left free to respond to any distortion resulting from weld deposition, as schematically shown in Fig. 3. During multipass GMA welding, the deflection of the free end of the weld joint per weld pass was measured using a dial gauge having least count of 0.01 mm placed at a given distance of 100 mm from weld centerline (L_C) — Fig. 3. The transverse shrinkage was measured at the center of the weld groove at a given strain length (L_S) (Ref. 2) of 100 mm — Fig. 3. After each pass of welding at any heat input, the transverse shrinkage and deflection of the plate from its initial position as well as the amount of weld deposition were measured, followed by an estimation of transverse shrinkage stress and bending stress using standard mathematical expressions below. The amount of weld deposition was estimated by measuring the weight gain of the plate after each weld pass. To maintain reliability in the study for weld characteristics, experiments were carried out on three to six welds for each welding parameter.

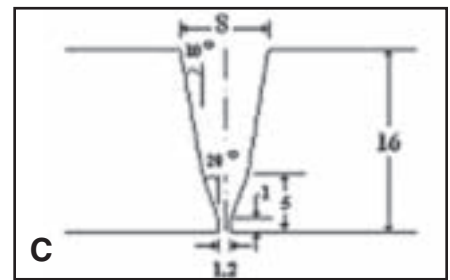
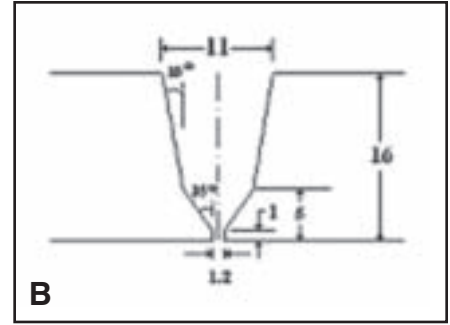


Fig. 2 — Schematic diagram of single (A) V-groove, (B) narrow groove of 11-mm opening (NG-11), and (C) narrow groove of 8-mm opening (NG-8).

Estimation of Heat Input (Ω)

The heat input (Ω) of GMAW and GMAW-P processes were estimated with consideration of the heat generated by the welding arc as a function of welding or mean current (I or I_m), arc voltage (V), welding speed (S), and its efficiency (η_a) as follows (Refs. 15, 16):

$$\Omega = \frac{\eta_a \times V \times [I(or)I_m]}{S} \quad (1)$$

The mean current (I_m) of the GMAW-P process may be expressed (Refs. 2, 17) as

$$I_m = \frac{(I_b t_b + I_p t_p)}{(t_b + t_p)} \quad (2)$$

The η_a of the GMAW process using mild steel filler metal under argon gas shielding has been considered as 70% (Ref. 18) whereas, according to the earlier statement, the η_a in the case of the GMAW-P process operating at different pulsed parameters has been worked out as a function of ϕ and I_m as follows (Ref. 19).

$$\eta_a = 94.52 - 0.118I_m - 107.61\phi$$

Table 1 — Chemical Composition (wt-%) of Base Metal

C	Si	Mn	Cr	Ni	Cu	Nb+Ti+V	Al	P	S
0.178	0.37	1.57	0.003	—	0.037	0.25 max	0.08	0.012	0.002

$$+ 0.348I_m\phi \quad (3)$$

Estimation of Total Heat Transferred to Weld Pool (Q_T)

The total heat transfer to the weld pool (Q_T) of the GMAW and GMAW-P processes was estimated (Ref. 12) with consideration of the arc heat transfer to the weld pool (Q_{AW}), heat of the filler metal transferred to the weld pool (Q_f), and welding speed (S) as follows.

$$Q_{rT} = \frac{(Q_{AW} + Q_f)}{S} \quad (4)$$

The Q_{AW} of the GMAW-P process is estimated as

$$Q_{AW} = (VI_{eff} - \psi I_{eff})\eta_a \quad (5)$$

Where ψ and I_{eff} are the effective melting potential at anode and effective current (root mean square value of the pulsed current wave form), respectively. The Q_{AW} of the GMAW process was estimated by substituting I_{eff} of Equation 5 with welding current (I). The I_{eff} is estimated (Refs. 2, 20) by the following expression:

$$I_{eff} = \sqrt{[k_p \cdot I_p^2 + (1-k_p) \cdot I_b^2]} \quad (6)$$

Where, the pulse duty cycle is

$$k_p = t_p/t_{pul} \quad (7)$$

The Q_f for the GMAW and GMAW-P processes was estimated (Refs. 12, 13, 17) as follows:

$$\text{For GMAW: } Q_f = Q_{de} m_t \quad (8)$$

$$\text{For GMAW-P: } Q_f = Q_{de} m_t f \quad (9)$$

Where m_t is mass of filler metal transferred per pulse (kg), Q_{de} is heat content per unit mass of the welding wire (Jkg^{-1}) at the time of deposition, and f is pulse frequency (Hz). The modeling detail for estimating Q_f of the GMAW-P process has been reported elsewhere (Refs. 12, 13).

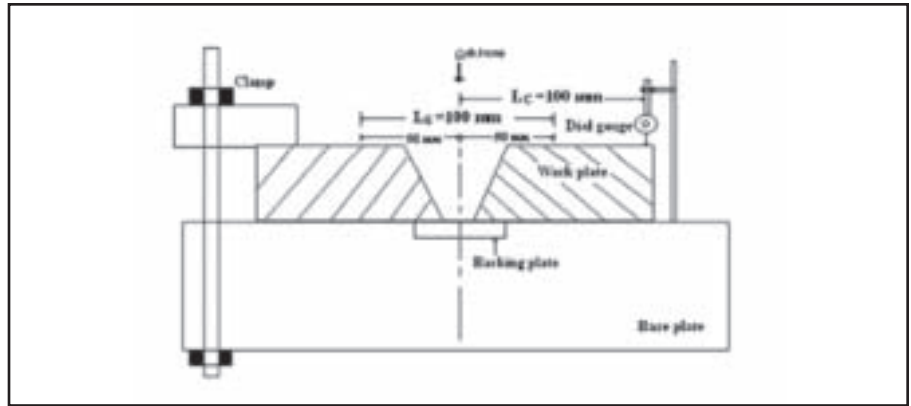


Fig. 3 — Schematic diagram of welding fixture.

The calorimetrically measured values of Q_{de} per unit mass of a deposited droplet in the GMAW process using 1.2-mm-diameter mild steel filler metal and covering the array of globular to spray metal transfer have been reported (Refs. 21, 22) by earlier workers.

Studies on Geometrical Characteristics of Weld Joint

A transverse section of the weld collected from the central part of the weld joint, assuring an area of stable welding, was polished by standard metallographic procedure and etched in 2% nital solution to reveal the weld geometry. Typical macrographs of the weld joints of V-groove, NG-11, and NG-8 produced by using the GMAW and GMAW-P processes are, respectively, shown in Fig. 4A–C and Fig. 5A–C. The geometrical characteristics of weld joint such as total area of weld deposit (A_{WD}) including the joint root opening (G), area of top (A_{TR}) and root (A_{RR}) reinforcement, area of base metal fusion (A_{BF}), and dilution ($\%D_L$) of base plate, as schematically shown in Fig. 6, was measured by graphical method. The estimation of A_{WD} , A_{BF} , and

D_L was carried out as follows:

$$A_{WD} = A_{WA} + A_{TR} + A_{BF} + A_{RR} \quad (10)$$

$$A_{BF} = A_{WD} - A_{WA} - A_{TR} - A_{RR} \quad (11)$$

$$\%D_L = \frac{A_{BF}}{A_{WD}} \times 100 \quad (12)$$

Estimation of Transverse Shrinkage Stress

The transverse shrinkage stress (σ_{tr}) developed in the weld joints during their preparation under the varied thermal behaviors of different welding processes, procedures, and parameters was estimated with the help of measured transverse shrinkage (Δ_{tr}) as follows (Refs. 2, 23):

$$\sigma_{tr} = \frac{R \times \Delta_{tr} \times E}{L_S} \quad (13)$$

Where E is the Young's modulus of base material ($210 \times 10^9 \text{ Nm}^{-2}$), R is the shape factor considered as 0.1 (Ref. 2), and L_S is the straining length of 100 mm (Fig. 3).

Estimation of Bending Stress

The bending stress (σ_b) developed through physically observed distortion of weld joints during their preparation under

Table 2 — Estimated Thermal Behavior of Welding at Different Parameters

Welding Process	Measured Welding Parameters										Estimated Thermal Behavior			
	V	S (cm/min)	$I^{(a)}/I_m$ (A)	ϕ	Pulse Parameters					Ω (kJ/cm)	Q_{AW} (J/s)	Q_{de} (J/kg)	Q_f (J/s)	Q_T (kJ/cm)
					I_p (A)	I_b (A)	f (Hz)	t_b (s)	t_p (s)					
GMAW	24±1	28	240±4 ^(a)	—	—	—	—	—	—	8.28 ± 0.5	2930	1834000	2156	10.89
			230±3	0.15	420	104	50	0.012	0.008	7.45 ± 0.4	4294	1755157	2059	13.61
GMAW-P	24	182±4	0.23	440	140	100	0.007	0.003	7.22 ± 0.5	4145	1702060	1996	13.16	
			0.15	372	88	100	0.006	0.004	7.1 ± 0.6	3789	1677370	1731	13.67	
			0.23	420	128	50	0.015	0.005	6.77 ± 0.5	3673	1625076	1677	13.38	



Fig. 4 — Typical macrograph of GMA weld joints having different sizes of weld grooves produced at a given Ω of 8.28 ± 0.5 kJ/cm. A — V-groove; B — NG-11; C — NG-8.



Fig. 5 — Typical macrograph of pulsed GMA weld joints having different sizes of weld grooves produced at a given $I_m = 230 \pm 3$ A, $\phi = 0.23$, and $\Omega = 7.22 \pm 0.5$ kJ/cm. A — V-groove; B — NG-11; C — NG-8.

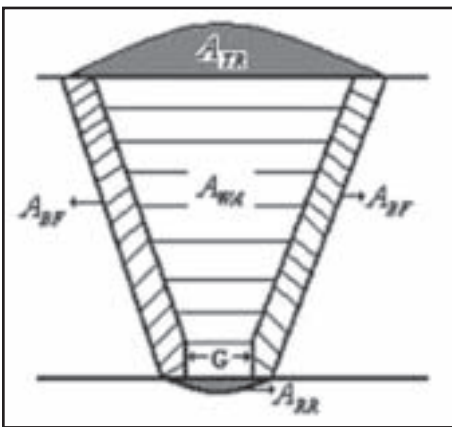


Fig. 6 — Schematic view of different locations of weld joint considered in graphical measurement of area of weld deposit (A_{WD}) and area of base metal fusion (A_{BF}).

varied thermal behavior of different welding processes and procedures was also estimated (Ref. 23) as follows:

$$\sigma_b = \frac{R \times M \times t}{2 \times I^m} \quad (14)$$

Where M is the bending moment, I^m is the moment of inertia, and t is plate thickness. The M and I^m are estimated (Ref. 23) as follows:

$$M = F \times L_C \quad (15)$$

$$I^m = \frac{b_w \times t^3}{12} \quad (16)$$

Where L_C is the distance of the measuring point (dial gauge tip, Fig. 3) from the central axis of the weld joint, and b_w is the plate width. The force (F) generated due to distortion of the plate was estimated (Ref. 23) with the help of measured deflection (δ) by considering it as a case satisfying cantilever beam theory in view of one end of the plate is fixed and other end is free to deflect as explained earlier (Fig. 3).

$$F = \frac{3\delta EI^m}{L_C^3} \quad (17)$$

The F has been appropriately estimated under different welding processes, procedures, and parameters.

Results and Discussion

GMAW

Geometrical Characteristics of Weld Joint

At a given heat input (Ω) of 8.28 ± 0.5 kJ/cm and a similar amount of weld deposition of 2.5 gm/cm per pass, the effect of welding procedure on geometrical characteristics of the weld with respect to its total area of weld deposit (A_{WD}), total area of base metal fusion (A_{BF}), and dilution of base metal (D_L) is shown in Fig. 7A–C. Figure 7A and B shows that the V-groove weld joint gives comparatively higher A_{WD} and A_{BF} than those of narrow groove weld joints. It may be due to the comparatively higher amount of weld deposition required in filling a V-groove weld joint than that of filling a narrow groove weld joint.

However, it is further observed that A_{BF} of the comparatively narrower weld joint (NG-8) is relatively higher than that of NG-11, but lower than V-groove weld joints. It is possibly attributed to a comparatively larger amount of base metal fusion on both sides of the groove wall in the root region of the narrower groove width of NG-8 than that of the V-groove and NG-11 welds at a given Ω and similar order of metal deposition. This may have caused more dilution of weld metal with base metal in the NG-8 weld compared to the NG-11 and V-groove weld joints as shown in Fig. 7C. The variation in extent of base metal fusion may also significantly affect the temperature of the weld pool and consequently its solidification behavior, influencing transverse shrinkage and deflection of weld joints.

Transverse Shrinkage Stress

At a given welding current (I) and heat input (Ω) of 230 ± 4 A and 8.28 ± 0.5 kJ/cm respectively, resulting in a similar rate of weld deposition (2.5 gm/cm), the effect of the number of weld passes on the cumulative transverse shrinkage (Δ_{tr}) measured during multipass GMA welding in different size grooves is shown in Fig. 8. The variation of results shown in the figure maintains a standard deviation (SD) lying in the range of ± 0.09 – 0.2 . The figure shows that at a given heat input the increase in the number of weld passes enhances the cumulative transverse shrinkage of the weld joint due to increase in the amount of weld metal deposition.

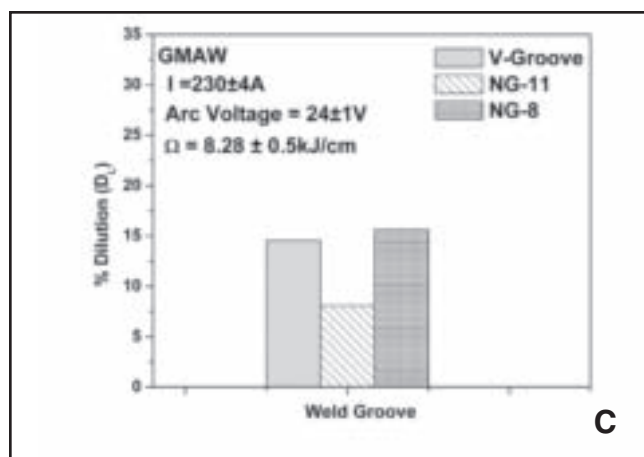
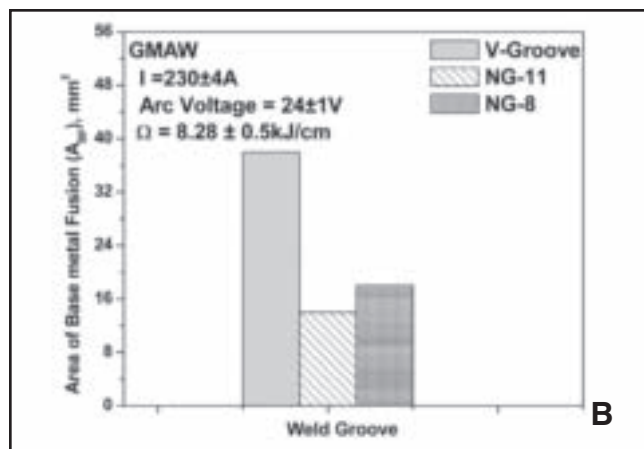
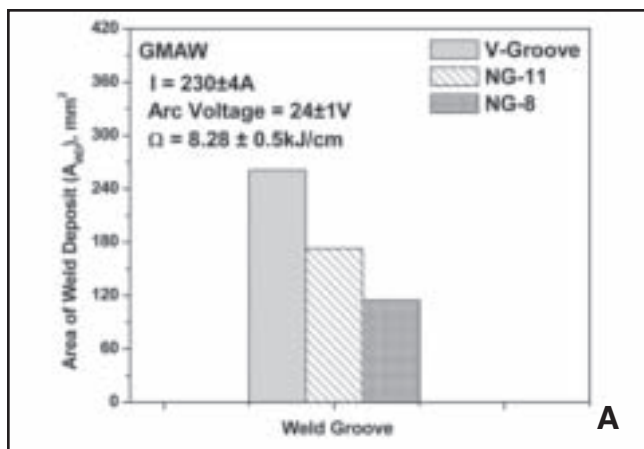


Fig. 7 — At a given Ω , $I_m\Omega$, and arc voltage, the effect of different weld grooves. A — Measured area of weld deposit; B — measured area of base metal fusion; C — dilution (%) of GMA weld deposit.

The figure further reveals that at a given Ω , the influence of weld pass on transverse shrinkage appreciably reduces as one proceeds from the root pass to subsequent filling passes. However, at a given weld pass, the cumulative shrinkage of the weld joint was found to be more in the NG-8 weld, but relatively less in the NG-11 weld with respect to that of the V-groove weld. On the basis of these observations, the change in estimated (Equation 13) transverse shrinkage stress (σ_{tr}) with the variation in weld groove size of GMA weld joint was studied and is shown in Fig. 9. The figure shows that the V-groove weld joint has a comparatively higher transverse shrinkage stress than that of the narrow groove weld joints, with the NG-11 weld having the lowest among them.

Deflection and Bending Stress

In line with the earlier observation (Fig. 8) on cumulative shrinkage (Δ_{tr}), the variation in cumulative deflection (δ) of the weld joint in the same range of given Ω and I with the increase in number of weld passes in multipass GMA weld deposition in different weld grooves was found to follow a similar trend as shown in Fig. 10. It was further observed that the δ gradually increases with the progress in number of weld passes from the root pass and at a given number of weld passes, it is relatively more in the NG-8 weld, but less in the NG-11 weld than that of the V-groove weld. On the basis of measured deflection of the weld joints as discussed above, it is a measure of bending of the plate from its neutral axis. At a given order of Ω , the effect of welding procedure on variation of shrinkage stresses in the weld deposit causing distortion of the weld joint can be corroborated by estimation of bending stress developed in the weld joint through measurement of degree of bending of the plate. This may provide a physical confirmation of the effect of welding process on the stress generation in the weld joint. At a given Ω , the effect of welding procedure

on estimated bending stress is shown in Fig. 11. It was observed that the estimated bending stress of narrow groove welds is always considerably lower than that of the V-groove weld. However, the estimated bending stress of the NG-11 was found to be marginally lower than that of the NG-8 weld, which is in agreement with the observed trend of estimated transverse shrinkage stress (Fig. 9) with respect to variation in groove size. In this context, it is further noted that the magnitude of the estimated transverse shrinkage lies in close approximation to the bending stress estimated on the basis of distortion generated in weld joints (Figs. 9 and 11) of different groove sizes.

GMAW-P

Geometrical Characteristics of Weld Joint

At a given I_m and close range of Ω of $230 \pm 3A$ and $7.22-7.45$ kJ/cm, respectively, and a similar amount of weld deposition of 2.5 gm/cm per pass, the effect of welding procedure using different weld grooves at varied ϕ of 0.15 and 0.23 on weld deposit, base metal fusion, and dilution of weld are shown in Fig. 12A–C. In agreement with those observed in GMAW, it was found that V-groove weld joints showed comparatively higher A_{WD} and A_{BF} but lower dilution than that of the narrow groove NG-8 weld joint. However, the NG-11 weld joint shows comparatively higher A_{WD} but lower A_{BF} and D_L than that of the NG-8 weld joint. It is also in-

terestingly observed that at a given Ω and I_m , the measures of aforesaid geometrical characteristics of all the V-groove, NG-11, and NG-8 weld joints reduce with the increase of ϕ . This may have primarily happened due to a decrease in total heat transfer to the weld pool (Q_T) (Table 2) with the increase of ϕ (Ref. 24). The lowering of Q_T with the increase of ϕ may reduce the weld groove shrinkage and A_{BF} , thus, decreases the A_{WD} and D_L . At a given welding or mean current (I or I_m), arc voltage, and welding speed, the Ω is relatively lower (Table 2) with GMAW-P than the GMAW process due to comparatively low process efficiency (η_a) of the former one causing rather low heat content per unit mass of the filler metal (Q_{de}) at the time of deposition. This behavior considerably reduces the A_{WD} , A_{BF} , and D_L of a pulsed GMA weld compared to the GMA weld at a higher ϕ of 0.23 , but at the same I_m , arc voltage, and welding speed, a decrease of ϕ to 0.15 makes the above-mentioned geometrical characteristics of the pulsed GMA weld comparable

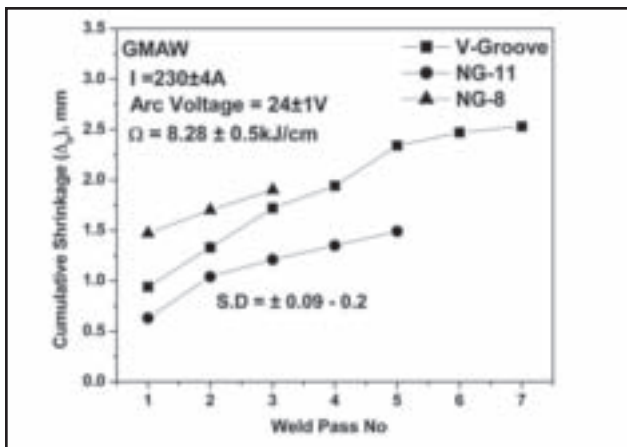


Fig. 8 — The effect of number of weld passes on measured cumulative transverse shrinkage during GMA weld deposition in different sizes of weld grooves at a given Ω , I_m , and arc voltage.

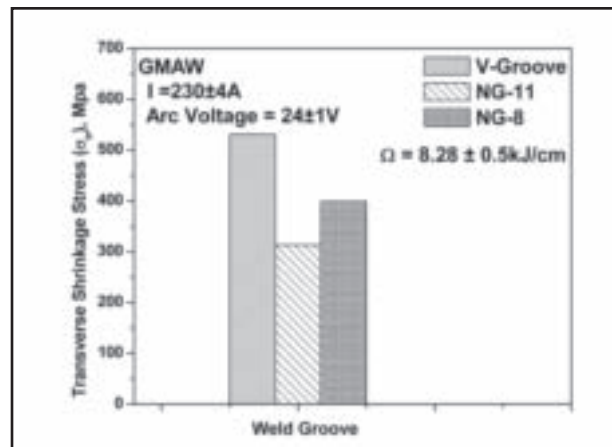


Fig. 9 — The effect of different weld grooves on estimated transverse shrinkage stress in GMA weld joints at a given Ω , I_m , and arc voltage.

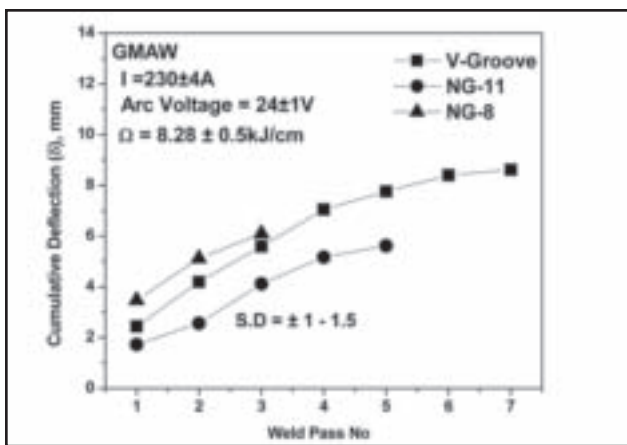


Fig. 10 — The effect of number of weld passes on measured cumulative deflection during GMA weld deposition in different sizes of weld groove at a given Ω , I_m , and arc voltage.

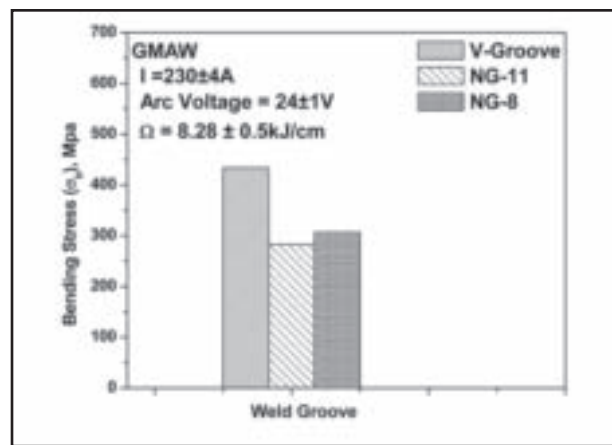


Fig. 11 — The effect of different weld grooves on estimated bending stress of GMA weld joints at a given Ω , I , and arc voltage.

to those of the GMA weld.

Similar observations on the variations in A_{WD} , A_{BF} , and D_L of the narrow groove NG-11 and NG-8 weld joints with a change in pulse parameters were noted as shown in Fig. 13A–C during welding at a relatively lower range of Ω and I_m of 6.77–7.1 kJ/cm and 182 ± 4A, respectively, with a weld deposition of 2.5 gm/cm per pass at different ϕ of 0.15 and 0.23. However, a comparison of Figs. 12 and 13 shows that at a given ϕ the A_{WD} , A_{BF} , and D_L of NG-11 and NG-8 weld joints reduces significantly with a decrease of I_m from 230 to 182 A. This may have primarily happened due to a comparatively low heat content per unit mass of weld deposition (Q_{de}) at lower I_m (Table 2), which can consequently make a difference in transverse shrinkage and deflection of the weld joint.

Transverse Shrinkage Stress

At a given I_m and close range of Ω of 230 ± 3 A and 7.22–7.45 kJ/cm, respectively, at different ϕ of 0.15 and 0.23, the effect of number of weld passes on cumulative transverse shrinkage (Δ_{tr}) measured during multipass pulsed GMA welding in different sized weld grooves is shown in Fig. 14. In order to maintain reliability in comparative observations on relatively small variations in Δ_{tr} , a statistical analysis was made. In agreement to the earlier observations on cumulative transverse shrinkage of the GMA weld joints at different weld groove sizes (Fig. 8), here also it was observed that the transverse shrinkage of the pulsed GMA weld joints increased with the increase of weld passes. However, at a given weld pass and similar order of I and I_m of about 230 A, the use

of GMAW-P in place of GMAW appreciably lowers the transverse shrinkage. In spite of a similar rate of weld deposition (2.5 gm/cm per pass), this may be primarily attributed to the phenomena of heat buildup (Refs. 5, 8, 25) with GMAW-P, which with the influence of interruption in metal deposition results in a comparatively milder thermal behavior of weld joints. At a given weld pass, the cumulative transverse shrinkage of the weld joint was found to be more in the NG-8 weld and relatively less in the NG-11 weld with respect to that of the V-groove weld. But, it was further observed that at a given I_m and Ω , the cumulative transverse shrinkage in all the V-groove, NG-11, and NG-8 weld joints reduced with the increase of ϕ — Fig. 14. This may have primarily happened due to the decrease in total heat transfer to the weld pool (Q_T) (Table 2) with the

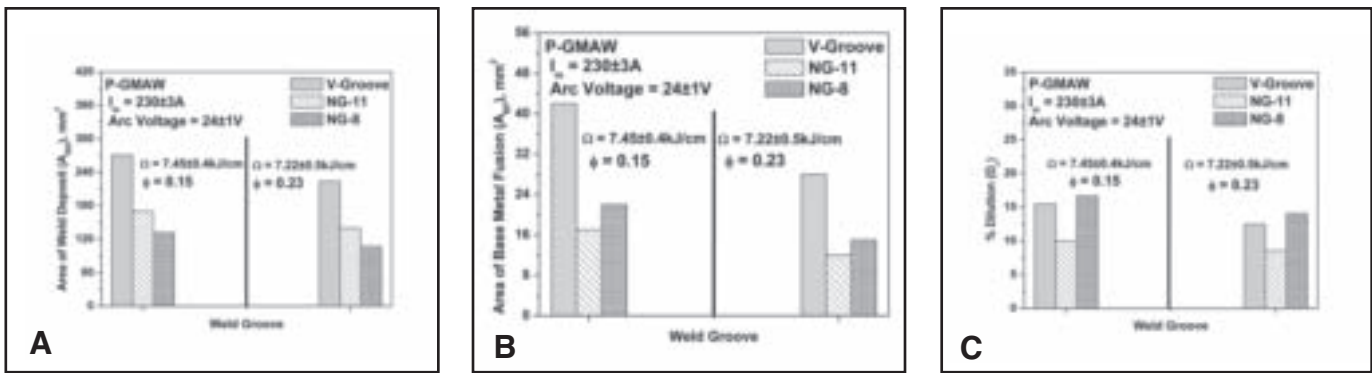


Fig. 12 — The effects of different weld grooves at a given Ω , I_m , and arc voltage of GMAW-P. A — Onmeasured area of weld deposit; B — area of base metal fusion; C — dilution of weld deposit.

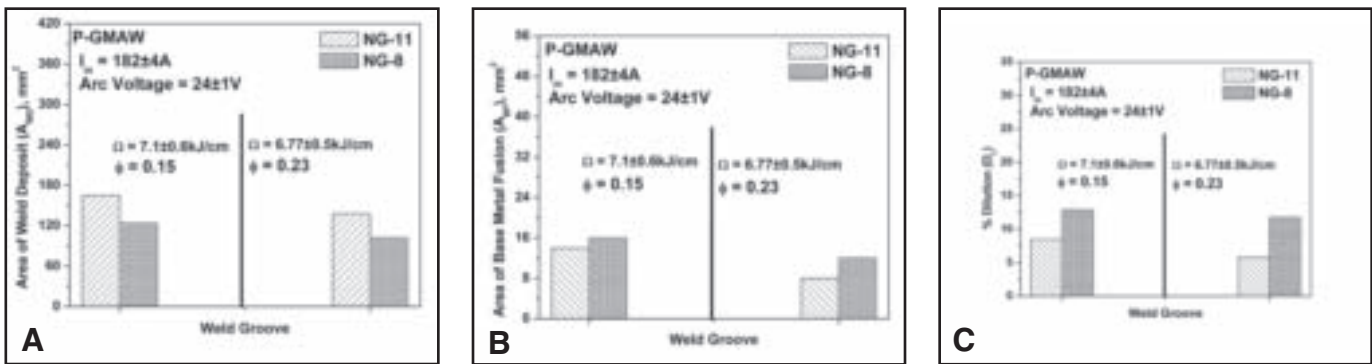


Fig. 13 — The effect of different weld grooves at a given relatively lower range of Ω and I_m of GMAW-P. A — On measured area of weld deposit; B — area of base metal fusion; C — dilution of weld deposit.

increase of ϕ as explained earlier. On the basis of these observations, the change in estimated (Equation 13) transverse shrinkage stress (σ_{tr}) with the variation in weld groove size of pulsed GMA weld joints at different ϕ has been studied as shown in Fig. 15. The figure shows that the V-groove weld joint is having comparatively higher transverse shrinkage stress than that of the narrow groove weld joints, where the NG-11 weld depicts the lowest shrinkage among them. However, Fig. 15 further shows that the transverse shrinkage stress developed in the weld joint prepared by the GMAW-P process with different weld groove sizes is comparatively lower than that observed in GMA weld joints — Fig. 9. This may be primarily attributed to the lower thermal intensity of the pulsed GMA weld due to a reduction in heat buildup in the weld deposit as a result of the interruption in weld deposition under pulsed current. It is interesting to note that at a given I_m and Ω , the transverse shrinkage stress of all the V-groove, NG-11, and NG-8 weld joints reduced with the increase of ϕ — Fig. 15.

At the comparatively lower range of I_m and Ω of 182 ± 4 A and 6.77–7.1 kJ/cm, respectively, the variation in cumulative transverse shrinkage with the increase of weld passes in different sizes of narrow groove welds observed at relatively lower and higher ϕ of 0.15 and 0.23 is shown in Fig. 16. In order to study the effect of I_m at different ϕ on transverse shrinkage of pulsed GMA welds, the observations in Figs. 14 and 16 were compared. It is observed that at a given ϕ , the decrease of I_m from 230 to 182 A at a close range of Ω significantly reduces the transverse shrinkage of both the NG-11 and NG-8 welds, possibly due to a comparatively low heat content per unit mass of the filler wire (Q_{dc}) at the time of deposition (Table 2) as explained earlier. The figures further depict that at a given I_m and Ω , the increase of ϕ relatively reduces the transverse shrinkage, especially in narrower weld NG-8. However, at a given weld pass, the cumulative shrinkage of the weld joint was found comparatively more with an NG-8 weld than with an NG-11 weld. On the basis of these observations, the varia-

tion in estimated (Equation 13) transverse shrinkage stress (σ_{tr}) with the change in groove size of pulsed GMA weld joints at relatively lower range of I_m and Ω at different ϕ was studied and is shown in Fig. 17. The figure shows that at a given ϕ of 0.15, the NG-8 weld has a comparatively higher transverse shrinkage stress than that of the NG-11 weld, whereas at the higher ϕ of 0.23, an opposite trend is observed. However, Fig. 17 further depicts that the transverse shrinkage stress developed in the weld prepared by GMAW-P using different weld groove sizes is comparatively lower than that observed (Fig. 15) in the pulsed GMA weld produced at relatively higher I_m and Ω of 230 ± 3 A and 7.22–7.45 kJ/cm, respectively. In view of the results depicted in Figs. 9, 15, and 17, the significant role different weld groove sizes plays on transverse shrinkage stress developed during welding is clearly understood, along with some further critical observations at varying Ω , I_m , and ϕ . It is noted that the NG-8 weld gives the lowest transverse shrinkage stress among all the welds of different groove sizes studied,

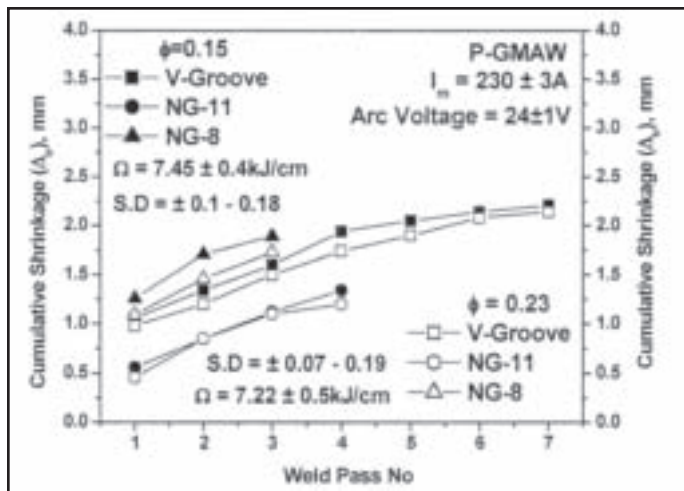


Fig. 14 — The effect of number of weld passes at a given Ω , I_m , and arc voltage of GMAW-P on measured cumulative transverse shrinkage of weld deposit under different sizes of weld groove at different ϕ .

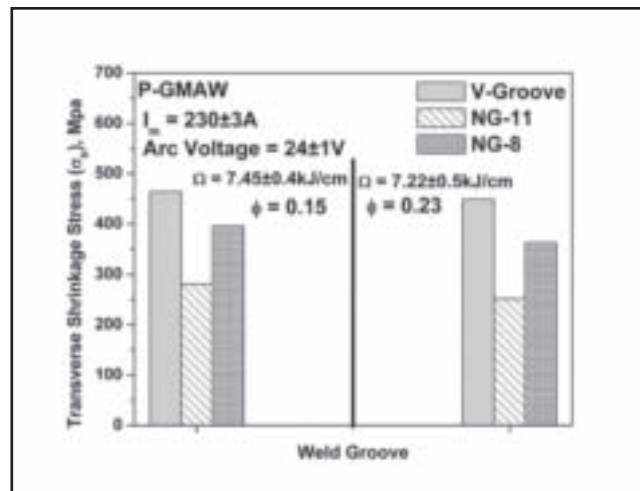


Fig. 15 — At a given Ω , I_m , and arc voltage of GMAW-P, the effect of different weld grooves on estimated transverse shrinkage stress of weld joints at different ϕ .

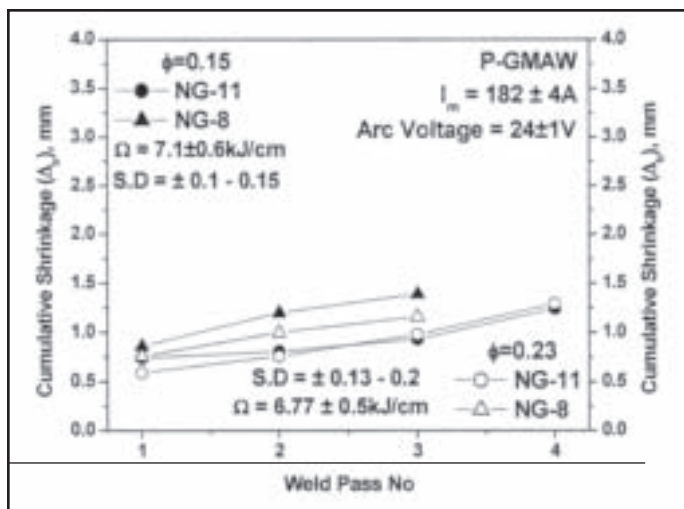


Fig. 16 — At a relatively lower range of Ω and I_m of GMAW-P, the effect of number of weld passes on measured cumulative transverse shrinkage of weld deposition in different sizes of weld groove at different ϕ .

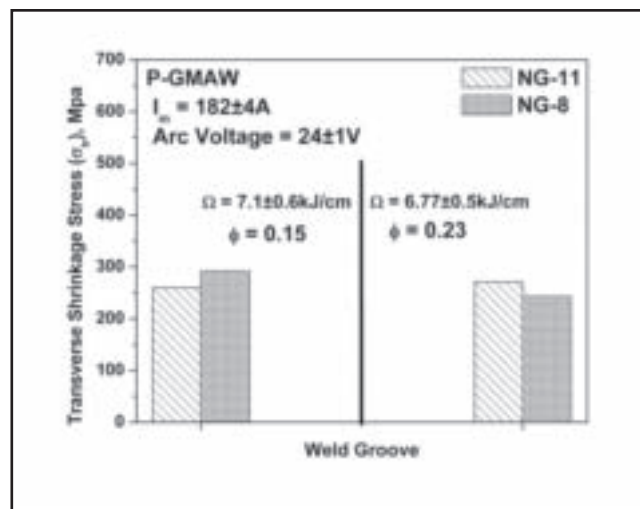


Fig. 17 — At a relatively lower range of Ω and I_m of GMAW-P, the effect of different weld grooves on estimated transverse shrinkage stress weld joints at different ϕ .

when a relatively higher ϕ of 0.23 is used at relatively lower range of I_m and Ω of 182 ± 4 A and $6.77-7.1$ kJ/cm, respectively. However, to have a clearer understanding of all the phenomena regarding the influence of welding process, procedure, and parameters on transverse shrinkage stress developed during welding, it should be studied further in detail using primarily more variation of ϕ at different groove sizes and plate thicknesses.

Deflection and Bending Stress

In line with earlier observation (Fig. 14) on cumulative shrinkage (Δ_{tr}), the variation in cumulative deflection (δ) of the

weld joint with an increase in number of weld passes using GMAW-P in different sized weld grooves in the same range of given Ω , I_m , and ϕ was found to follow a similar trend as shown in Fig. 18 for different ϕ of 0.15 and 0.23, respectively. The figure shows that the deflection developed in the weld joint prepared by GMAW-P, especially at higher ϕ of 0.23, is significantly lower than that observed (Fig. 10) in the GMA weld joint prepared with similar current voltage and heat input. This may be primarily understood by the comparatively lower estimated shrinkage stress (Fig. 15) of the pulsed GMA weld deposit, which generates comparatively lower bending force in the weld joint as a result

of relatively smaller heat buildup than that noted (Fig. 11) in the GMA weld joint. However, at a given weld pass, the cumulative deflection of the weld joint was found to be more with the NG-8 weld, but relatively less with the NG-11 weld with respect to the V-groove weld. It was further observed that at a given Ω and I_m , the cumulative deflection of the weld joint with all the V-groove, the NG-11 and NG-8 welds reduced with the increase of ϕ — Fig. 18. At a given range of I_m and Ω of 230 ± 3 A and $7.22-7.45$ kJ/cm, respectively, and a different ϕ of 0.15 and 0.23, the effect of welding procedure on bending stress developed in the weld joint estimated (Equation 14) on the basis of

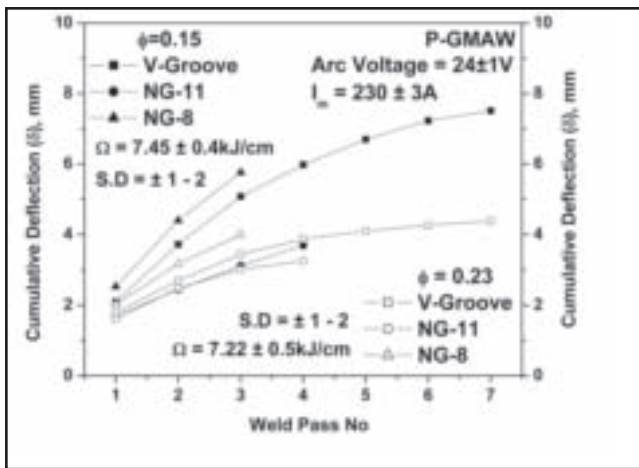


Fig. 18 — At a given Ω , I_m and arc voltage of GMAW-P, the effect of number of weld passes on measured cumulative deflection of weld deposition under different sizes of weld groove at different ϕ .

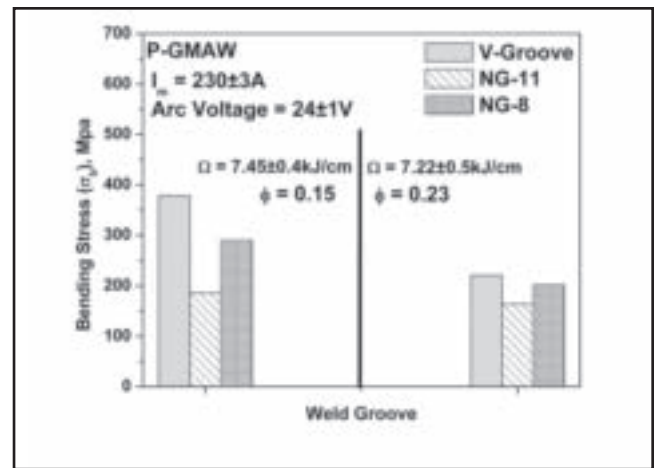


Fig. 19 — At a given Ω , I_m and arc voltage of GMAW-P, the effect of different weld grooves on estimated bending stress of weld joints at different ϕ .

measured bending during multipass pulsed GMA welding in different weld groove sizes is shown in Fig. 19. It was observed that the estimated bending stress is marginally lower in the NG-11 weld than the NG-8 weld, but in both cases it is considerably lower than the V-groove weld, which follow a similar trend of estimated transverse shrinkage stress — Fig. 15. In this context, it was further corroborated that the estimated transverse shrinkage is well in agreement to the bending stress estimated on the basis of distortion generated in weld joints — Figs. 15 and 19.

At the comparatively lower range of I_m and Ω of 182 ± 4 A and 6.77–7.1 kJ/cm, respectively, the increase in cumulative deflection with the increase of weld passes in different sizes of narrow grooves observed at relatively lower and higher ϕ of 0.15 and 0.23 is shown in Fig. 20. The figure shows a similar trend of variation in transverse shrinkage as explained earlier (Fig. 16) in the case of variation in cumulative shrinkage under the same conditions of welding. But, it is observed that at any ϕ , the cumulative deflection is marginally lower in NG-11 than NG-8 weld. However, it was noted that at a given ϕ , the decrease of I_m from 230 to 182 A reduces the deflection significantly, and the effect is comparatively more with NG-11 weld as revealed in Figs. 18 and 20, respectively. On the basis of these observations, the variation in estimated (Equation 14) bending stress (σ_{tr}) with the change in weld groove size of pulsed GMA weld joints at the relatively lower range of I_m and Ω at different ϕ was studied as shown in Fig. 21. In line with earlier observations on the change in transverse shrinkage stress (Fig. 17) with an increase of ϕ under the same conditions of welding, a similar trend was ob-

served concerning bending stress of the weld joints especially at a lower ϕ of 0.15.

In view of the above discussions regarding transverse shrinkage stress and bending stress generated under different welding processes and weld groove sizes, it is understood that the NG-8 weld develops comparatively higher transverse shrinkage stress and bending stress than the NG-11 weld, especially at higher thermal influence of more Ω or lower ϕ (Refs. 12, 13, 25). This may have happened due to a comparatively larger proportion of groove filling during the root pass deposition in the comparatively narrower groove of NG-8 than NG-11 weld — Fig. 23. Accordingly, the force (F_R) generated in the weld contributing to development of bending moment (M_R) in the groove wall causing its distortion resulting from root pass deposition in different sizes of weld grooves using different welding processes have been estimated by using Equations 15 and 17, respectively. The variation in F_R and M_R with respect to the welding process, groove size, and welding parameters is shown in Fig. 22 A and B, respectively. The figure shows that through the root pass the NG-8 weld generates relatively higher F_R and M_R than that observed with the V-groove and NG-11 weld joints, where the NG-11 weld is the lowest among them. Mechanism of the force (F_R) and bending moment (M_R) generated during root pass weld for V-grooves as well as NG-11 and NG-8 grooves is schematically shown in Fig. 23A–C. Figure 23 clearly shows that a decrease in weld groove size significantly enhances the proportionate filling of the weld groove by root pass, adversely affecting the shrinkage stress and bending stress of the weld. However, this phenomenon has to be studied further in order to exploit the use of narrow groove

welding of thick plates with appropriate amount of weld deposition per pass.

Conclusions

The investigation revealed that the use of GMAW-P in multipass butt joining of thick (16-mm) steel plate is beneficial to reduce the shrinkage stress of the weld deposit as well as distortion and bending stress of the weld joint compared to using conventional GMAW at a given welding heat input. During GMAW-P at a given heat input, a control of pulse parameters gives rise to a relatively higher ϕ and further improves the weld characteristics in this regard. The use of a narrow weld groove instead of a conventional V-groove also improves the situation in this respect. The variation of weld characteristics in question with a change of pulse parameters primarily happens due to decrease in total heat transfer (Q_T) to the weld pool as a function of the transfer of arc heat (Q_{AW}) and heat of the filler metal (Q_f) to it with a change in ϕ at a given welding speed (S), where the increase of ϕ decreases the Q_T . The change in said weld characteristics with groove size is largely dictated by the amount of weld deposit. However, the use of a too narrow weld groove, where the root pass can fill the groove more than half of its depth, may restrict the beneficial effect of narrow groove to minimize the bending stress of weld joint.

Acknowledgments

The author thankfully acknowledges

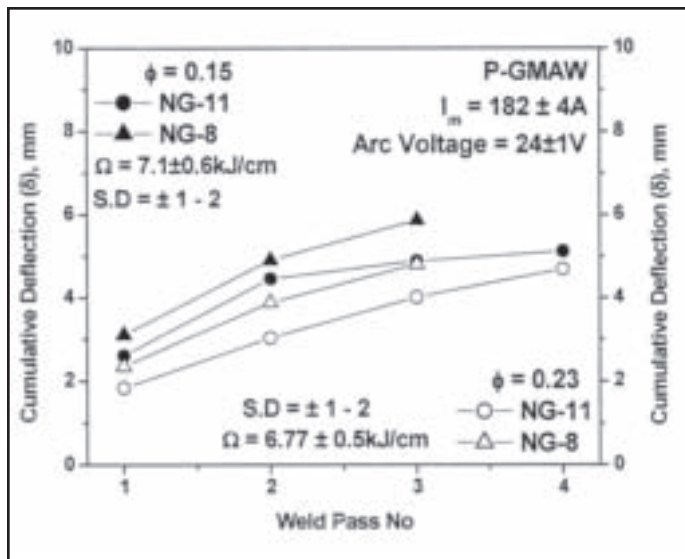


Fig. 20 — At a relatively lower range of Ω and I_m of GMAW-P effect of number of weld passes on measured cumulative deflection of weld deposition in different sizes of weld groove at different ϕ .

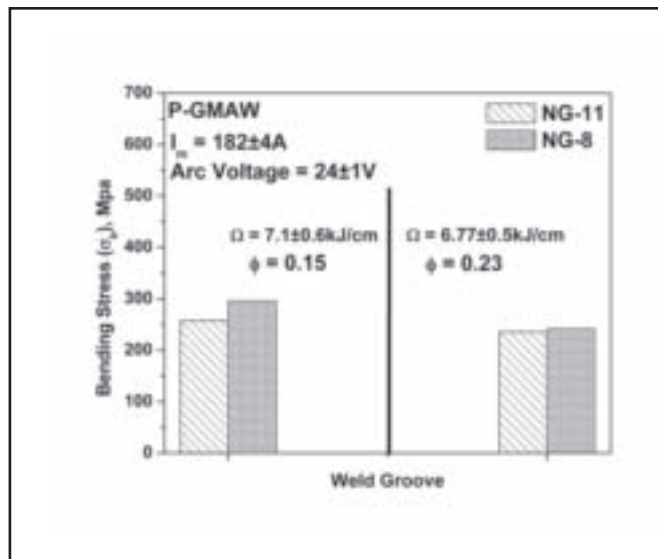


Fig. 21 — At a relatively lower range of Ω and I_m of GMAW-P effect of different weld grooves on estimated bending stress of weld joint at different ϕ .

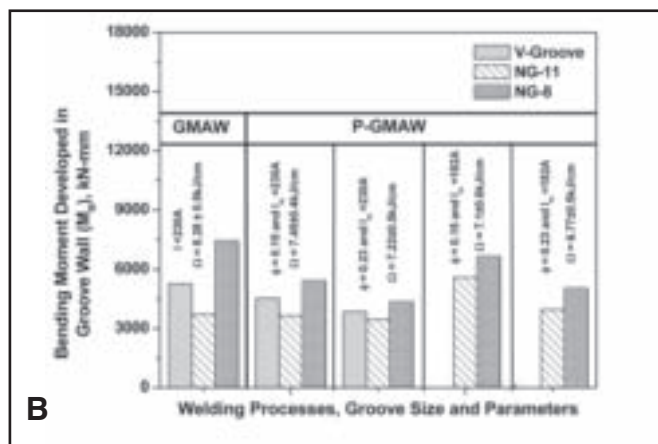
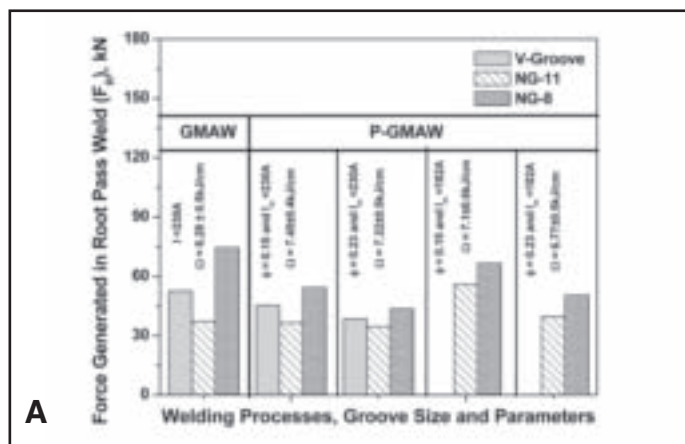


Fig. 22 — Effect of root pass deposition using different welding processes and weld groove sizes. A — Force (F_R) generated in weld; B — bending moment (M_R) developed in groove wall.

the Council of Scientific and Industrial Research (CSIR), India, and for financial support to K. Devakumaran, research associate during analysis of the work.

References

1. Masubuchi, K. 1980. *Analysis of Welded Structures*. New York, Pergamon Press, p. 235.
2. Radaj, D. 1992. *Heat Effects of Welding*. Berlin, Springer-Verlag, p. 182.
3. Parmer, R. S. 1997. *Welding Engineering and Technology*. New Delhi, Khanna Publishers, p. 214.
4. Teng, T.-L., and Chang, P.-H. 2004. Effect of residual stresses on fatigue crack initiation life for butt welded joints. *J Mater Process Technol* (145): 325–335.

5. Ghosh, P. K., and Ghosh, A. K. 2004. Control of residual stresses affecting fatigue life of pulsed current gas metal arc weld of high-strength aluminum alloy. *Met. Mater. Trans. A* (35A): 2439–2446.
6. Deng, D., and Murakawa, H. 2008. Prediction of welding distortion and residual stress in a thin plate butt welded joint. *Comp Mater Sc* (43): 353–365.
7. Deng, D., Murakawa, H., and Liang, W. 2008. Numerical and experimental investigations on welding residual stress in multi pass butt welded austenitic stainless steel pipe. *Comp Mater Sc* (42): 234–244.
8. Kulkarni, S. G., Ghosh, P. K., and Ray, S. 2008. Improvement of weld characteristics by variation in welding processes and parameters in joining of thick wall 304LN stainless steel pipe. *ISIJ Int.* (48): 1560–1569.

9. Sattari Far, I., and Javadi, Y. 2008. Influence of welding sequence on welding distortions in pipes. *Int J Pressure Vessel and Piping* (85): 265–274.
10. Tang, T. L., and Lin, C. C. 1998. Effect of welding conditions on residual stresses due to butt weld. *Int J of Pressure Vessel and Piping* (75): 857–864.
11. Panin, V. N. 2007. Experimental calculation estimation of residual welding distortion in shells of turbine penstocks at hydraulic power stations. *The Paton Welding J*, pp. 7–11.
12. Goyal, V. K., Ghosh, P. K., and Saini, J. S. 2008. Analytical studies on thermal behavior and geometry of weld pool in pulsed current gas metal arc welding. *J Mater Process Technol* (209): 1318–1336.
13. Ghosh, P. K., Goyal, V. K., Dhiman, H. K., and Kumar, M. 2006. Thermal and metal

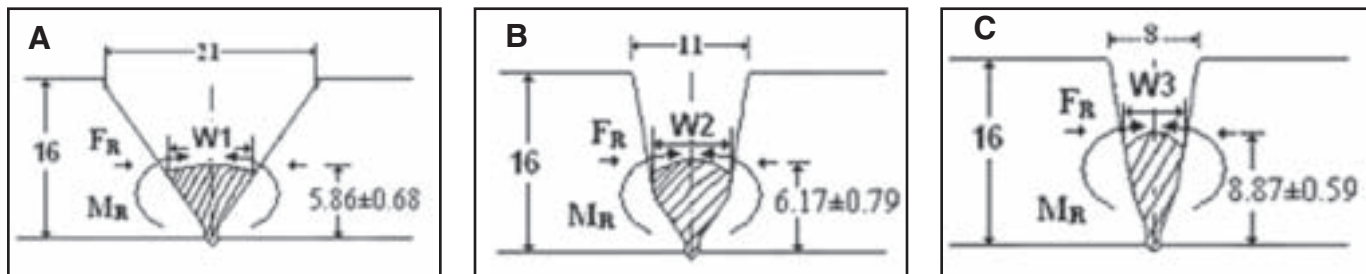


Fig. 23 — Schematic diagram showing the proportionate filling of groove with the root pass contributing to force generated and bending moment developed in weld with different groove sizes. A — V-groove; B — NG-11; C — NG-8.

transfer behavior in pulsed current GMA weld deposition of Al-Mg alloy. *Sci. Technol. Weld. Joining* 11(2): 232–242.

14. Ghosh, P. K., Randhawa, H. S., and Gupta, S. R. 2000. Characteristics of a pulsed-current vertical up gas metal arc weld in steel. *Met. Mater. Trans. A* 31A(12): 2247–2259.

15. Jenney, C. L., and O'Brien, A., eds. 2001. *AWS Welding Handbook*. 9th ed. Vol. 1, p. 110, American Welding Society, Miami, Fla.

16. Messler, Jr., R. W. 1999. *Principles of Welding*. New York, John Wiley & Sons, p. 181.

17. Lancaster, J. F. 1984. *The Physics of Welding*. New York, International Institute of Welding, p. 109.

18. Christensen, N., de L. Davis, V., and Gjermundsen, K. 1965. Distribution of temperature in arc welding. *British Welding J* 12(2): 54–75.

19. Ghosh, P. K., Devakumaran, K., and Bhaskarijyoti, S. 2009. Arc efficiency in pulsed current gas metal arc welding of ferrous and non ferrous materials. *Australian Welding J.*, 4th quarter.

20. Joseph, A., Harwig, D., Farson, D., and Richardson, R. 2003. Measurement and calculation of arc power and heat transfer efficiency in pulsed gas metal arc welding. *Sci. Technol. Weld. Joining* 8(6): 400–406.

21. Essers, W. G., and Walter, R. 1981. Heat transfer and penetration mechanisms with GMA and plasma GMA welding. *Welding Journal* 60(2): 37-s to 42-s.

22. Ueguri, S., Hara, K., and Komura, H. 1985. Study of metal transfer in pulsed GMA welding. *Welding Journal* 64(8): 242-s to 250-s.

23. Khurmi, R. S. 2002. *Strength of Materials*. 467, India, S. Chand & Company.

24. Goyal, V. K., Ghosh, P. K., and Saini, J. S. 2008. Influence of pulse parameters on characteristics of bead on plate weld deposits of aluminium and its alloy in P-GMA welding process. *Met. Mater. Trans. A* (39A): 3260–3275.

25. Ghosh, P. K., Ravi Reddy, M., and Devakumaran, K. 2006. Distortion and transverse shrinkage stress in butt welds of steel plates under different welding procedure and parameters of GMAW and SMAW processes. *Indian Welding J.* 38(4): 15–23.

Nomenclature

Symbol	Description
A_{WD}	Total area of weld deposit (mm^2)
A_{WA}	Initial area of weld groove (mm^2)
A_{TR}	Area of top reinforcement (mm^2)
A_{BF}	Area of base metal fusion (mm^2)
A_{RR}	Area of root reinforcement (mm^2)
b_w	Plate width (mm)
D_L	Dilution (%)
E	Young's modulus (MPa)
F	Force generated due to distortion (N)
F_R	Force generated at the root pass weld due to distortion (N)
f	Pulse frequency (Hz)
G	Root opening (mm)
I	Welding current (A)
I_{eff}	Effective current (A)
I_p	Peak current (A)
I_b	Base current (A)
I_m	Mean current (A)
I_m	Moment of inertia (mm^4)
k_p	Pulse duty cycle
L_S	Straining length (mm)
L_C	Distance of the measuring point (mm)
M	Bending moment (N-mm)
M_R	Bending moment developed in groove wall (kN-mm)
m_t	Mass of filler metal transferred per pulse (kg)
Q_T	Total heat transferred to weld pool (kJ/cm)
Q_{AW}	Arc heat transferred to the weld pool (Js^{-1})
Q_{de}	Heat content per unit mass of the filler metal at the time of deposition (J kg^{-1})
Q_f	Heat of the filler metal transferred to the weld pool (Js^{-1})
R	Shape factor
S	Welding speed (m/min)
SD	Standard deviation
t	Thickness of the base plate (mm)
t_p	Pulse on time (s)
t_b	Pulse off time (s)
V	Arc voltage (V)
ϕ	Summarized influence of pulse parameters factor
η_a	Arc efficiency (%)
ψ	Effective melting potential at anode (mild steel = 5.8 V)
Ω	Heat input (kJ/cm)
σ_{tr}	Transverse shrinkage stress (MPa)
σ_b	Bending stress (MPa)
Δ_{tr}	Measured transverse shrinkage (mm)
δ	Measured deflection (mm)

Dear Readers:

The *Welding Journal* encourages an exchange of ideas through letters to the editor. Please send your letters to the Welding Journal Dept., 550 NW LeJeune Rd., Miami, FL 33126. You can also reach us by FAX at (305) 443-7404 or by sending an e-mail to Kristin Campbell at kcampbell@aws.org.